

GLOBAL ENERGETICS ANALYSIS USING 3-DIMENSIONAL  
NORMAL MODE DECOMPOSITION

Hiroshi Tanaka and Ernest C. Kung

University of Missouri-Columbia

Columbia, Mo. 65211

## 1. INTRODUCTION

The normal modes are the eigen-solutions of linearized primitive equations over a sphere, and the 3-dimensional normal mode functions (3-D NMF) are obtained for a motionless atmosphere by solving the vertical and the horizontal structure equations. Since Kasahara and Puri (1981) first obtained the orthonormal eigensolutions to the vertical structure, it became possible to decompose the atmospheric energy into the 3-D NMF. Tanaka (1985) developed a diagnostic global energetics scheme using the 3-D NMF (hereafter called normal mode energetics scheme) which not only analyzes the three dimensional energy spectra but also examines energy transformations in and among the 3-D NMF.

The normal mode energetics scheme involves more assumptions than the standard spectral energetics diagnosis (e.g., Kung and Tanaka, 1983; Saltzman, 1957). The 3-D NMF are obtained for a basic state at rest. Despite its restrictions, there are specific advantages of this scheme. The energetic characteristics of the various vertical and horizontal modes, such as the barotropic, baroclinic, Rossby, and gravity modes can be examined separately. The normal mode energetics is likely suitable for the high frequency gravity waves, Kelvin waves and mixed Rossby-gravity waves in the tropics and the fast moving external Rossby waves in the middle latitude to which the influence of the zonal wind is small. Therefore, the normal mode energetics will be a useful diagnostic tool to supplement the standard spectral energetics analysis of the general circulation.

In this study the normal mode energetics scheme is applied to the Goddard Laboratory for Atmospheric Sciences (GLAS) analysis data of the FGGE observation for a 25-day period in January 1979. The results of the energetics analysis are compared with those of the Geophysical Fluid Dynamics Laboratory (GFDL) analysis for three winter months by

Tanaka (1985). The utilities of the normal mode energetics scheme are examined.

## 2. DATA AND ANALYSIS SCHEME

The GLAS analysis data cover a 25-day period, 5 through 29 January 1979. Daily grid-point values of horizontal wind speed  $u$ ,  $v$ , vertical  $p$ -velocity  $\omega$ , geopotential height  $\phi$ , temperature  $T$  and humidity  $q$  are given at 1000, 850, 700, 500, 400, 300, 250, 200, 150, 100, 70 and 50 mb at 0000 GMT. The objective analysis scheme to produce the GLAS analysis data set is described by Baker (1983). The basic state for the vertical eigenfunction was computed separately from the analysis data for 5 January - 5 March and 1 June 31 July 1979.

The spectral representation of dimensionless primitive equations using 3-D NMF as a basis of expansion function may be written as

$$\frac{d}{dt} w_{srm} - i\sigma_{srm} w_{srm} = b_{srm} + c_{srm} + d_{srm}, \quad (1)$$

where  $i^2 = -1$ , and the complex value  $w_{srm}$  represents an expansion coefficient of dependent variable vector of  $(u \ v \ \phi)$ ,  $b_{srm}$  that of nonlinear term vector due to wind field,  $c_{srm}$  due to mass field,  $d_{srm}$  that of a vector due to diabatic process and  $\sigma_{srm}$  the dimensionless eigenfrequency as a solution of the horizontal (Laplace's tidal) equation. The Rossby mode and the eastward and westward propagating gravity modes are distinguished using  $\sigma_{srm}$ . The subscripts  $s$ ,  $r$ , and  $m$ , respectively denote zonal wavenumber, meridional mode index and vertical mode index for the expansion. The vertical mode  $m=0$  is regarded as the barotropic mode and  $m \geq 1$  as the baroclinic modes.

The corresponding energy balance equation with dimensional form is given by

$$\frac{d}{dt} E_{srm} = B_{srm} + C_{srm} + D_{srm}, \quad (2)$$

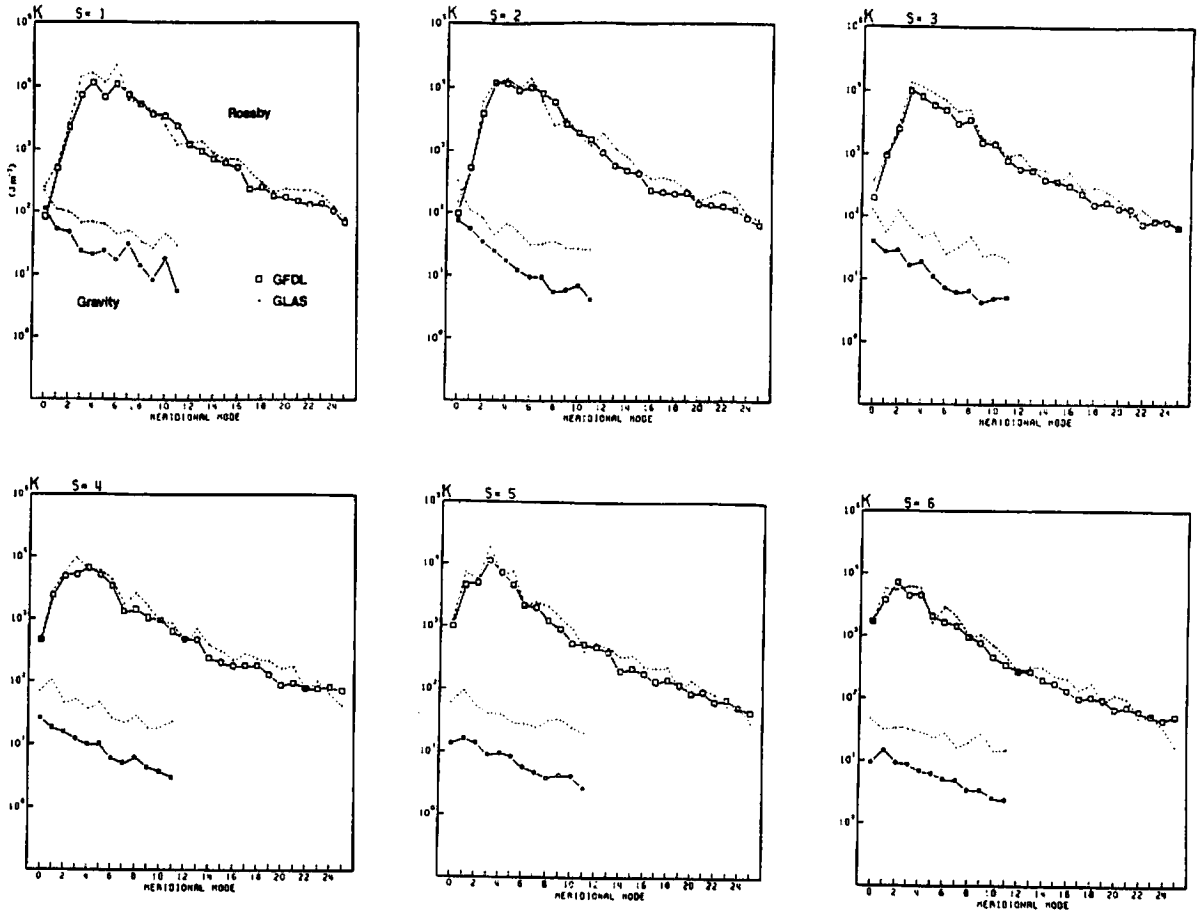


Fig. 1 Kinetic energy spectra of barotropic mode ( $m=0$ ) in the meridional mode domain for zonal wavenumber  $s=1$  through 6.

where

$$E_{sr m} = \frac{1}{2} p_s h_m |w_{sr m}|^2. \quad (3)$$

$$B_{sr m} = p_s \Omega h_m [w_{sr m}^* b_{sr m} + w_{sr m} b_{sr m}^*]. \quad (4)$$

$$C_{sr m} = p_s \Omega h_m [w_{sr m}^* c_{sr m} + w_{sr m} c_{sr m}^*]. \quad (5)$$

$$D_{sr m} = p_s \Omega h_m [w_{sr m}^* d_{sr m} + w_{sr m} d_{sr m}^*]. \quad (6)$$

The asterisk denotes complex conjugate,  $p_s$  the global mean surface pressure,  $h_m$  the equivalent height and  $\Omega$  the angular speed of the earth's rotation. The time change of a normal mode energy  $E_{sr m}$  is caused by the nonlinear mode-mode interaction of kinetic energy  $B_{sr m}$ , that of available potential energy  $C_{sr m}$  and energy source or sink due to the diabatic process  $D_{sr m}$ . The kinetic energy  $K_{sr m}$  and available potential energy  $A_{sr m}$  are retrieved by  $E_{sr m}$  using vector norms of Hough functions. It may be readily demonstrated that the summations of interaction terms,  $B_{sr m}$  and  $C_{sr m}$ , respectively becomes zero. These energetics terms are computed and averaged for the 25 day data period.

### 3. RESULTS

The kinetic energy spectra of barotropic mode ( $m=0$ ) in the meridional mode domain are shown in Fig. 1 for wavenumber  $s=1$  through 6. For both the GLAS and GFDL analyses, the energy

spectra of Rossby modes indicate clear energy peaks at the meridional mode  $r=2$  (for  $s=6$ ) to  $r=6$  (for  $s=1$ ). For higher indices beyond these energy peaks, the spectra approximately follow the  $-3$  power of the meridional mode index. The energy levels drop rapidly at the lowest indices. We may say the two energy spectra by the GLAS and GFDL coincide with each other as far as the Rossby modes are concerned. It is shown in our separate ongoing study, using an eigenvalue problem of linear primitive equations, that the energy distributions and peaks in the meridional mode domain are attributable to the properties of the baroclinic instability about the zonally-varying basic state. On the other hand, the energy spectra of gravity modes approximately obey the  $-5/3$  power for both the GLAS and GFDL analyses despite the different treatment of the gravity mode, i.e., the Euler-backward time integration for the GLAS analysis and the global optimum interpolation with the nonlinear normal mode initialization for the GFDL analysis (Daley et al., 1985). However, the energy levels of the GLAS analysis are apparently higher than those of the GFDL analysis. Quantitatively, the eddy kinetic energy ( $s=1-15$ ) of barotropic gravity modes for the GLAS analysis ( $5.84 \cdot 10^3 \text{ Jm}^{-2}$ ) is more than threefold larger than that for the GFDL analysis ( $1.86 \cdot 10^3 \text{ Jm}^{-2}$ ).

Since a Hough function is associated with an eigenfrequency, we attempted to investigate the energy spectra in the frequency domain utilizing the eigenfrequency as a coordinate. The results are illustrated in Fig. 2 for the barotropic

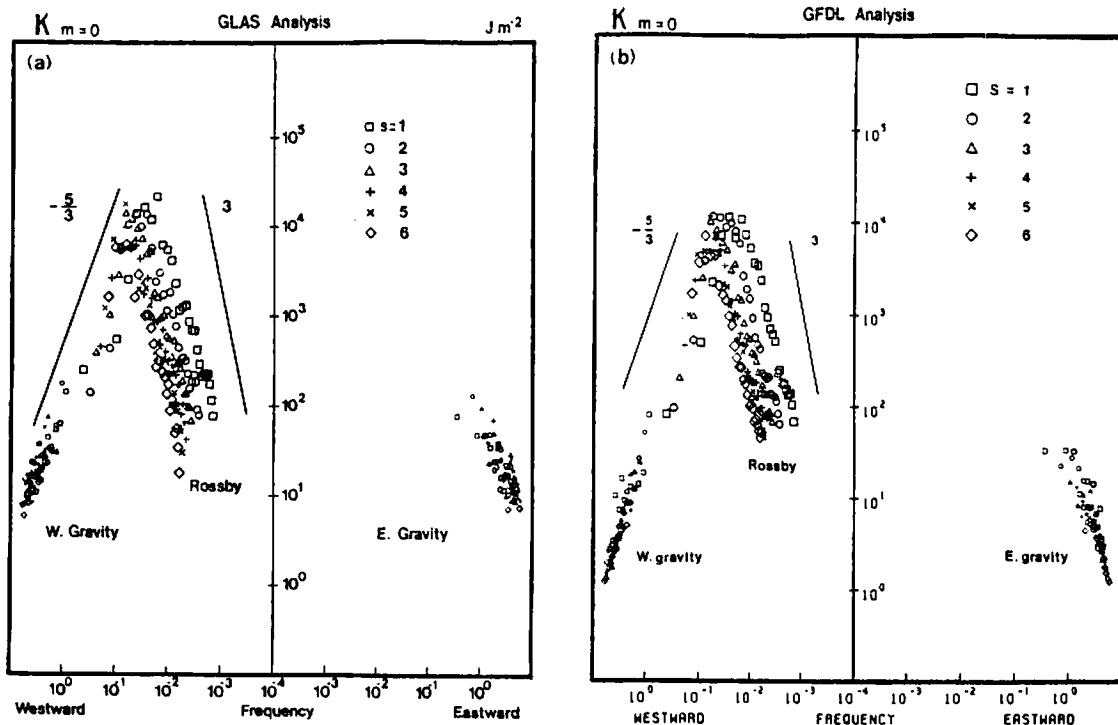


Fig. 2 Kinetic energy spectra of barotropic mode ( $m=0$ ) in the frequency domain for (a) GLAS and (b) GFDL analyses. Large symbol: Rossby mode, Small symbol: gravity mode.

kinetic energy of westward propagating Rossby and gravity modes and eastward propagating gravity modes. Energy peaks appear at the frequency of  $\sigma=0.03$  (for  $s=1$ ) to  $\sigma=0.07$  (for  $s=6$ ) corresponding to the energy peaks in Fig. 1. The energy spectra of low frequency Rossby modes follow approximately the 3 power of the frequency as is deduced from Fig. 1 with the Rossby-Haurwitz dispersion relationship. Similarly, the spectra of the gravity modes obey the  $-5/3$  power law. The most interesting features of this result are that the energy spectra of high frequency Rossby modes not only seem to follow the  $-5/3$  power law, but also merge continuously with the spectra of the gravity modes. The mixed Rossby-gravity modes ( $r=0$  in Fig. 1) are positioned between the two types of modes. These features are common for the GLAS and GFDL analyses except the relatively higher energy levels of gravity modes by the GLAS analysis.

Synthesizing energy interactions of the Rossby mode over all wavenumbers and meridional modes, we have the energy flow among the vertical modes. In Fig. 3 the total diabatic process is presented as a function of the vertical mode. This term is evaluated as the residual of the energy balance equation (2), taking account of the time change of the energy. The total diabatic process ( $s=0-15$ ) is separated into zonal ( $s=0$ ) and eddy ( $s=1-15$ ) contributions. Despite the different vertical structures of the eigensolutions between the GLAS and GFDL analyses, the qualitative comparison may be informative. Both the GLAS and GFDL analyses indicate energy generation in the baroclinic modes ( $m=2-4$ ) and dissipation at the barotropic mode ( $m=0$ ). The separation of the total diabatic process into zonal and eddy components reveals a significant difference between the two analyses in the zonal

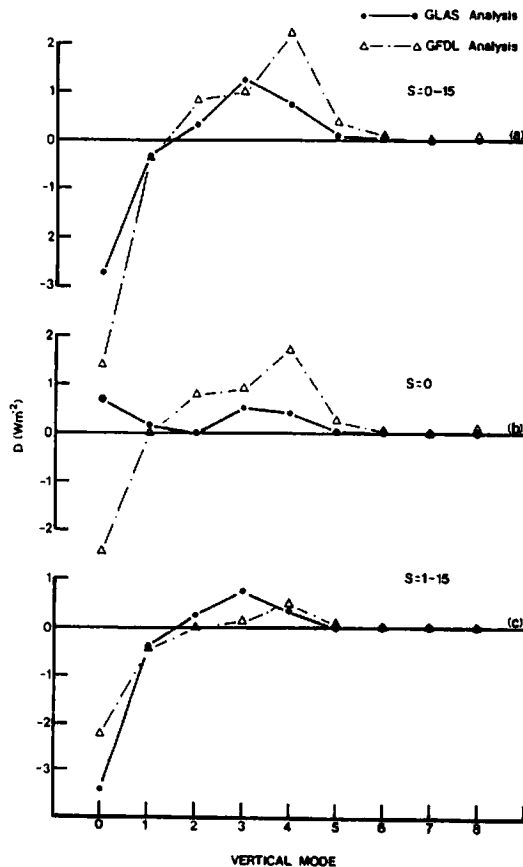


Fig. 3 Energy generation (positive) and dissipation (negative) as a function of the vertical mode. (a): total, (b): zonal mean, (c): eddy.

Table 1. Energy and energy balance of the zonal mean (s=0) and eddy (s=1-15) components for barotropic (m=0) and baroclinic (m=1-11) decompositions. Units are  $10^5 \text{ Jm}^{-2}$  for kinetic energy (K), available potential energy (A) and total energy (E), and  $\text{Wm}^{-2}$  for interaction of kinetic energy (B), available potential energy (C) and total diabatic process (D).

Data and mode	K	A	E	B	C	D
GLAS analysis						
s=0 m=0	7.1	2.1	9.2	0.64	-1.29	0.69
m=1-11	3.7	48.1	51.8	0.07	-1.08	1.13
s=1-15 m=0	4.8	2.8	5.0	0.62	2.71	-3.42
m=1-11	4.7	4.8	9.5	-1.18	0.19	0.94
GFDL analysis						
s=0 m=0	6.4	1.9	8.3	0.50	1.96	-2.46
m=1-11	4.2	48.6	52.8	-0.05	-3.96	4.05
s=1-15 m=0	3.6	0.2	3.8	0.34	1.86	-2.20
m=1-11	4.2	4.0	8.2	-0.99	0.58	0.37

field. The GFDL analysis shows a large energy generation in the baroclinic mode and large dissipation at the barotropic mode, but the generation is small in the baroclinic modes and the barotropic mode is also a generation for the GLAS analysis. For eddies, however, the characteristics of the energy generation in the baroclinic modes and the dissipation at the barotropic mode are similar for the GLAS and GFDL analyses.

The budgets of the normal mode energetics analysis are summarized in Table 1 including the energy transformations. Contributions from the gravity modes are excluded from the values. The energy levels are in good agreement between the GLAS and GFDL analyses. The computed energy transformations from zonal to eddy are 1.66 and 1.55 ( $\text{Wm}^{-2}$ ) for the GLAS and GFDL analyses, respectively, and the transformations from baroclinic to barotropic modes are 2.68 and 4.66 ( $\text{Wm}^{-2}$ ). These values are comparable with the diagnosis by Kung and Tanaka (1983). Although both of the GLAS and GFDL analyses indicate energy generation in the baroclinic modes and dissipation in the barotropic mode, the intensity of the energy transformations shows nearly twofold difference between the two analyses. The difference is attributed to the generation in the barotropic mode of zonal field for the GLAS analysis in contrast with the energy sink for the GFDL analysis.

#### 4. CONCLUDING REMARKS

There are significant differences between the GLAS and GFDL analyses data in a barotropic energy of gravity modes. By the GLAS analysis the energy level of this mode is more than three times larger than that by the GFDL analysis. Another substantial difference is noted in the energy transformations of the zonal mean field. By the GLAS analysis the barotropic mode of zonal mean field indicates a energy generation, whereas that by the GFDL analysis is a large energy sink. Overall, however, we may see a general agreement

in the 3 power and -5/3 power laws of energy spectra in low and high frequency ranges, and energy balance between the generation in baroclinic mode and dissipation in barotropic mode. The present study may demonstrate utilities of the three-dimensional normal mode energetics as a diagnostic tool.

#### ACKNOWLEDGMENT

This research was supported by the NOAA Grant NA83AA-D-00052. The analysis of GLAS data was performed at ECK Research Consulting, Inc. under NASA Contract NA55-28116.

#### REFERENCES

- Baker, W. E. 1983: Objective analysis and assimilation of observational data from FGGE. *Mon. Wea. Rev.*, 111, 328-342.
- Daley, R., A. Hollingsworth, J. Ploshay, K. Miyakoda, W. Baker, E. Kalnay, C. Dey, T. Krishnamurti, and E. Barker, 1985: Objective analysis and assimilation techniques used for the production of FGGE IIIb analyses. *Bull. Amer. Meteor. Soc.*, 66, 532-538.
- Kasahara, A., and K. Puri, 1981: Spectral representation of three-dimensional global data by expansion in normal mode functions. *Mon. Wea. Rev.*, 109, 37-51.
- Kung, E. C., and H. Tanaka, 1983: Energetics analysis of the global circulation during the special observation periods of FGGE. *J. Atmos. Sci.*, 39, 2575-2592.
- Saltzman, B. 1957: Equations governing the energetics of the larger scales of atmospheric turbulence in the domain of wave number. *J. Meteor.*, 14, 513-523.
- Tanaka, H. 1985: Global energetics analysis by expansion into three-dimensional normal mode functions during FGGE winter. *J. Meteor. Soc. Japan*, 63, 180-200.